HHS Public Access

Author manuscript

Nat Immunol. Author manuscript; available in PMC 2014 November 01.

Published in final edited form as:

Nat Immunol. 2014 May ; 15(5): 465–472. doi:10.1038/ni.2866.

Protein Kinase C-η Controls CTLA-4-Mediated Regulatory T Cell Function

Kok-Fai Kong[1,*,†], **Guo Fu**[2,*,†], **Yaoyang Zhang**[3], **Tadashi Yokosuka**[4], **Javier Casas**[2], **Ann J. Canonigo-Balancio**[1], **Stephane Becart**[1], **Gisen Kim**[5], **John R. Yates III**[3], **Mitchell Kronenberg**[5], **Takashi Saito**[4], **Nicholas R. J. Gascoigne**[2,6,*,‡,§], and **Amnon Altman**[1,*,‡]

[1]Division of Cell Biology, La Jolla Institute for Allergy and Immunology, La Jolla, California, USA

[2]Department of Immunology and Microbial Science, The Scripps Research Institute, La Jolla, California, USA

[3]Department of Chemical Physiology, The Scripps Research Institute, La Jolla, California, USA

[4]RIKEN Center for Integrative Medical Sciences, Yokohama, Japan

[5]Division of Developmental Immunology, La Jolla Institute for Allergy and Immunology, La Jolla, California, USA

[6]Department of Microbiology, Yong Loo Lin School of Medicine, National University of Singapore, Singapore

Abstract

Regulatory T cells (T_{reg} cells), which maintain immune homeostasis and self-tolerance, form an immunological synapse (IS) with antigen-presenting cells (APCs). However, signaling events at the T_{reg} IS remain unknown. Here we show that protein kinase C-η (PKC-η) associated with CTLA-4 and was recruited to the T_{reg} IS. PKC-η-deficient T_{reg} cells displayed defective suppressive activity, including suppression of tumor immunity but not autoimmune colitis. Phosphoproteomic analysis revealed an association between CTLA-4-PKC-η and the GIT-PIX-PAK complex, an IS-localized focal adhesion complex. Defective activation of this complex in PKC-η-deficient T_{reg} cells was associated with reduced CD86 depletion from APCs by T_{reg} cells. These results reveal a novel CTLA-4-PKC-η signaling axis required for contact-dependent suppression, implicating this pathway as a potential cancer immunotherapy target.

*Correspondence should be addressed to: Amnon Altman (amnon@liai.org), Nicholas R. J. Gascoigne (michead@nus.edu.sg), Kok-Fai Kong (kfkong@liai.org).

†These authors contributed equally.

‡These authors share senior authorship.

§Current address: Yong Loo Lin School of Medicine, National University of Singapore, Singapore

Author Contributions

K.F.K. and G.F. designed experiments, collected data, performed analyses and wrote the paper; J.C., T.Y. and T.S. performed microscopy experiment; A.J.C. was involved in experiments and data collection; S.B. performed and assisted in melanoma studies; Y.Z. and J.Y. did the phosphoproteomic experiment and analyses; G.K. and M.K. provided critical reagents and were involved in study design; N.R. J.G. and A.A. designed the study, analyzed data and wrote the paper.

The authors declare no competing financial interests.

The discovery and recognition of $CD4^+Foxp3^+$ T_{reg} cells as a distinct subset of T cells with immunoregulatory function represents a major advance in our understanding of the immune system[1-3]. T_{reg} cells actively maintain immune homeostasis and self-tolerance, and one prominent T_{reg} cell-mediated suppressive mechanism is dependent upon contact with antigen presenting cells (APCs)[4]. This physical contact promotes the formation of a specialized signaling platform, known as the immunological synapse (IS), at the T_{reg} cell-APC interface.

CTLA-4 is a potent negative regulator of T cell-mediated immune responses through its actions in both T_{eff} and T_{reg} cells. CTLA-4 is highly expressed on T_{reg} cells[3], and this high expression, as well as the higher affinity of CTLA-4 for its CD80 (B7-1) and CD86 (B7-2) ligands by comparison with CD28[5] is associated with predominant localization of CTLA-4 at the T_{reg} cell IS and, consequently, displacement of CD28 from the IS[6]. However, despite extensive studies on CTLA-4, little is known about the intracellular signaling pathways initiated upon CTLA-4 engagement by its ligands. The SHP1, SHP2 and PP2A phosphatases, which represent binding partners of CTLA-4[7], may account for the intrinsic inhibitory activity of CTLA-4 in T_{eff} cells, but a recent study demonstrated that these phosphatases are not recruited to the T_{reg} cell IS together with CTLA-4[6]. Thus, how CTLA-4 exerts its signaling effects at the T_{reg} cell IS remains unknown.

The T_{reg} cell IS is distinguishable from the “conventional” IS formed between naïve or effector T (T_{eff}) cells and APCs in several respects. First, although the TCR is present in the central supramolecular activation cluster (cSMAC) in both types of IS, the costimulatory CD28 receptor is recruited to the T_{eff} IS, whereas CTLA-4 is present at the T IS[6, 8]. Second, PKC-θ is absent from the T_{reg} cell IS and, moreover, in contrast to T_{eff} cells, it negatively regulates the function of T_{reg} cells[4]. Physical association of PKC-θ, mediated by its V3 domain, with the costimulatory CD28 receptor underlies its cSMAC recruitment and essential functions in driving the activation, proliferation and differentiation of T_{eff} cells[9]. Hence, the absence of PKC-θ in the T_{reg} cell IS suggests that TCR signaling events in these cells could differ significantly from those of T_{eff} cells. Nevertheless, proximal TCR signaling appears intact in T_{reg} cells, as indicated by the phosphorylation and activation of TCR, Lck[10], PDK1[11], LAT and PLCγ1[12], all of which have been implicated in the *in vitro* suppressive function of T_{reg} cells. Because of these findings and, in particular, the importance of the association between LAT and activated PLCγ1[12], which is required for the hydrolysis of phosphatidylinositol 4,5-bisphosphate (PIP_2) and generation of diacylglycerol (DAG), the PKC-activating second messenger, we hypothesized that DAG should be produced locally[13] upon IS formation in T_{reg} cells and, furthermore, that this would lead to the IS recruitment and activation of a PKC family member other than PKCθ, which may positively regulate the function of T_{reg} cells.

Here we show that, by analogy with the PKC-θ-CD28 interaction in T_{eff} cells, which promotes their activation and function[9], the CD28-related receptor CTLA-4, which is highly expressed on T_{reg} cells and is required for their suppressive function[14, 15], physically recruits another member of the novel PKC (nPKC) subfamily, PKC-η, which localizes at the T_{reg} cell IS following stimulation. This association required phosphorylated serine residues in PKC-η and a conserved, membrane-proximal motif in the cytoplasmic tail of CTLA-4,

respectively. Although T_{reg} cell development and the expression of typical T_{reg} cell markers were normal in PKC-η-deficient (*Prkch*$^{-/-}$) T_{reg} cells, these cells displayed a grossly impaired contact-dependent suppressive activity *in vitro* and *in vivo*, which was associated with a grossly defective activation of NFAT and NF-κB. Lastly, we show that defective activation of a focal adhesion complex consisting of p21-activated kinase (PAK) and two additional proteins, PIX and GIT2, which was physically associated with CTLA-4 and PKC-η, was associated with reduced ability of *Prkch*$^{-/-}$ T_{reg} cells to serially engage APCs, thereby providing a potential mechanistic basis for the impaired suppressive activity of these cells. Therefore, strategies that interfere with this novel signaling pathway may be beneficial for inhibiting T_{reg} cell function in cancer and, hence, boosting the immune response against tumors.

RESULTS

Phospho-PKC-η interacts with CTLA-4 and is recruited to the T_{reg} cell IS

By analogy to the interaction of PKC-θ with the CTLA-4-related costimulatory receptor, CD28, which is critical for the activation of T_{eff} cells[9], we first tested if any PKC isoform could physically interact with CTLA-4. Using T hybridoma cells, we found that CTLA-4 coimmunoprecipitated with a higher than normal molecular weight (MW) species of PKC-η (Fig. 1a), but not with any other T cell-expressed PKC isoforms (Supplementary Fig. 1a). We reasoned that the MW shift of PKC-η might be a result of its phosphorylation. Indeed, alkaline phosphatase treatment partially reversed the shift of the higher MW species of PKC-η and resulted in the appearance of a lower MW species (Fig. 1b), indicating that CTLA-4 interacts predominantly with phosphorylated PKC-η. Consistently, phospho-PKC-η was found in unstimulated Foxp3^{+} T_{reg} cells, but not in naïve T cells (Fig. 1c), despite the fact that PKC-η protein expression was not significantly different between T_{eff} and T_{reg} cells (Supplementary Fig. 1b). Using a T_{reg} cell-APC conjugation system and confocal microscopy, we observed that, relative to PKC-θ, PKC-η was preferentially localized in the T_{reg} cell IS, where it was partially colocalized with the TCR (Fig. 1d). We analyzed the relative intensity of the PKC-η or PKC-θ fluorescence signals in the T_{reg} cell IS by calculating the intensity ratio in the IS *vs*. the opposite T cell pole. About 15% (3/20) of imaged cells displayed preferential localization of PKC-θ in the IS (ratio ≥ 5), consistent with the observation that a similar percentage of cells in this population were FoxP3^{-} (by intracellular staining), representing contaminating activated T_{eff} cells in the iT_{reg} culture. Among the remaining cells, the intensity ratios for PKC-η and PKCθ were 2.84 ± 0.22 and 1.51 ± 0.18 ($P < 0.0001$), respectively (data not shown). Taken together, these results indicate that phospho-PKC-η associates with CTLA-4 in T_{reg} cells and, furthermore, that PKC-η preferentially colocalizes with CTLA-4 in the IS.

Development of Foxp3^{+} T_{reg} cells is independent of PKC-η

Given the critical role of CTLA-4 in contact-dependent T_{reg} cell suppressive function, which involves depletion of CD80 and CD86 from APCs[14, 15], we next examined the CD4^{+}Foxp3^{+} T_{reg} cell population in the lymphoid organs of *Prkch*$^{-/-}$ mice by intracellular Foxp3 staining. The number and frequency of CD4^{+}Foxp3^{+} cells was not significantly altered in the thymi and spleens of *Prkch*$^{-/-}$ mice compared to wild-type mice (Fig. 2a, b and Supplementary

Fig. 2a). However, there was a consistent increase in the numbers of $CD4^+Foxp3^+$ T_{reg} cells in the peripheral (pLN) and mesenteric (mLN) lymph nodes of these mice (Fig. 2c, d), suggesting that PKCη is dispensable for the *in vivo* development of $CD4^+Foxp3^+$ T cells. Phenotypically, cells that have been "licensed" to become $Foxp3^+$ expressed similar levels of typical T_{reg} cell markers, including Foxp3, TCR-β chain, CTLA-4, CD25, glucocorticoid-induced tumor necrosis factor receptor (GITR) and CD44 (Fig. 2e-j). Thus, PKC-η is dispensable for nT_{reg} cell development *in vivo*, and for iT_{reg} cell differentiation *in vitro* as assessed by expression of typical T_{reg} cell markers.

PKC-η is required for $Foxp3^+$ T_{reg} cell suppressive function

We next explored the possibility that PKC-η might be required for the suppressive function of $Foxp3^+$ T_{reg} cells. To enable definitive identification of T_{reg} cells, we crossed *Prkch*$^{-/-}$ mice with mice coexpressing Foxp3 and enhanced GFP under the control of the endogenous *Foxp3* promoter (*Foxp3-IRES-eGFP*, hereafter called FIG)[16] to generate *Prkch*$^{-/-}$-FIG mice. We sorted $CD4^+GFP^+$ T_{reg} cells from wild-type and *Prkch*$^{-/-}$ FIG mice, and found that, upon stimulation, they produced similar amount of interleukin 10 (IL-10) (Fig. 2k), a cytokine that can mediate the suppressive activity of T_{reg} cells[17, 18].

We next considered the possibility that, despite the presence of an apparently normal T_{reg} cell population in *Prkch*$^{-/-}$ mice, the suppressive activity of these cells may be defective. We first used a conventional *in vitro* T_{reg} cell suppression assay, which assessed the proliferation of naïve T cells cocultured with T_{reg} cells and stimulated with anti-CD3 plus splenic dendritic cells (DCs) as an APC source. The percentage of dividing T_{eff} cells was consistently higher in cultures with *Prkch*$^{-/-}$ T_{reg} cells compared to T_{eff} cells cocultured with wild-type T_{reg} cells (Fig. 3a). The *Prkch*$^{-/-}$$T_{reg}$ cells were substantially impaired in their ability to suppress the proliferation of T_{eff} cells even at high T_{reg}/T_{eff} cell ratios, indicating that PKC-η expression by T_{reg} cells is important for their function.

To demonstrate the importance of PKC-η in T_{reg} cell function *in vivo*, we used two distinct experimental models, namely, homeostatic T cell expansion and tumor growth. Transfer of naïve $CD4^+$ $CD62L^+$ T cells into immune deficient mice leads to their massive proliferation, a process generally referred to as homeostatic expansion, although it is likely that some of this proliferation is antigen driven[19]. T_{reg} cells control the expansion of T_{eff} cells in a lymphopenic environment[20]. Purified naïve $CD45.1^+CD4^+$ T cells, either alone or in the presence of sorted wild-type or *Prkch*$^{-/-}$ $CD45.2^+CD4^+GFP^+$ T_{reg} cells, were adoptively transferred into *Rag1*$^{-/-}$ mice, and T cell numbers were determined one week post-transfer. In the presence of wild-type T_{reg} cells, $CD45.1^+$ T_{eff} cell expansion was significantly reduced in all secondary lymphoid organs examined; in contrast, minimal or no reduction in T_{eff} cell expansion was observed in the presence of *Prkch*$^{-/-}$ T_{reg} cells (Fig. 3b-d). Similar numbers of wild-type and *Prkch*$^{-/-}$ T_{reg} cells were present in these tissues (Supplementary Fig. 2b).

We next investigated the ability of *Prkch*$^{-/-}$ T_{reg} cells to inhibit the immune response against a growing tumor. Splenocytes depleted of $CD25^+$ T cells were adoptively transferred into *Rag1*$^{-/-}$ mice as a source of T_{eff} cells in the absence or presence of T_{reg} cells one day prior to inoculation of B16-F10 melanoma cells[14, 21]. Transfer of $CD25^+$-depleted

splenocytes alone resulted in relatively small skin tumors, whereas mice receiving T_{eff} cells together with wild-type T_{reg} cells developed massive B16 tumors, reflecting inhibition of the T_{eff} cell anti-tumor response by the cotransferred T_{reg} cells (Fig. 3e). Cotransfer of *Prkch*$^{-/-}$ T_{reg} cells resulted in substantially reduced tumor growth similar to that seen in mice receiving only T_{eff} cells (Fig. 3e). Taken together, these results indicate that in the absence of PKC-η, the *in vivo* suppressive function of T_{reg} cells is attenuated, leading to enhanced homeostatic proliferation and anti-tumor immunity.

Consistent with the importance of PKC-η in T_{reg} cell suppressive functions, *Prkch*$^{-/-}$ mice exhibit lymphadenopathy, reflected by increased T and B cell numbers, as well as a higher proportion of CD44^{hi} T cells, characteristic of an activated phenotype[22]. Indeed, *Prkch*$^{-/-}$ CD44^{hi} T cells secreted significantly elevated amounts of effector cytokines, including IL-2, IFN-γ, IL-4 and IL-17A (Fig. 4a-d), upon *in vitro* stimulation with anti-CD3 plus -CD28 monoclonal antibodies (mAbs). Consistent with this hyperactive phenotype, *Prkch*$^{-/-}$ mice displayed elevated serum levels of IgE (Fig. 4e) and autoantibodies against double-stranded DNA and histone (Fig. 4f, g, respectively) at 8-12 weeks of age, implying a deregulated, hyperactive immune system in the absence of PKC-η.

We also assessed the ability of wild-type and *Prkch*$^{-/-}$ T_{reg} cells to inhibit the development of autoimmune colitis in an established in a T cell transfer model. While the transfer of naïve wild-type T cells alone into *Rag1*$^{-/-}$ recipient mice induced weight loss, indicative of the development of chronic inflammatory bowel disease, cotransfer of either wild-type or *Prkch*$^{-/-}$ GFP^{+} T_{reg} cells protected the recipients against weight loss (Supplementary Fig. 3a) and inhibited the expansion of T_{eff} (CD45.1^{+}) cells (Supplementary Fig. 3b). Thus, despite the *in vitro* (Fig. 3a) and *in vivo* (Fig. 3b-e) severe defects in their suppressive function, *Prkch*$^{-/-}$ T_{reg} cells were still able to protect, albeit perhaps incompletely, recipient mice against the development of colitis. This finding suggests that in this particular disease model, *Prkch*$^{-/-}$ - cells employ an alternative, PKCη-independent suppressive mechanism(s), *e.g.*, IL-10-mediated suppression (Fig. 2k). Furthermore, increased proliferation (or localization) of *Prkch*$^{-/-}$ T_{reg} cells in the inflammatory bowel environment may compensate for their defective intrinsic suppressive function. Indeed, greater numbers of cotransferred *Prkch*$^{-/-}$ T_{reg} cells relative to wild-type T_{reg} cells were found in the secondary lymphoid organs of the recipient mice, and this effect tended to be more pronounced in the mLNs, which drain the site of inflammation (Supplementary Fig. 3c). Together, these findings suggest that PKC-η is not globally required for all forms of T_{reg} cell-induced suppression, and that it is dispensable for T_{reg}-mediated inhibition of colitis

Mapping and biological significance of CTLA-4-PKC-η interaction sites

The predominant association of phospho-PKC-η with CTLA-4 in T_{reg} cells suggested that phosphorylated residues mediate this interaction. To pinpoint potential phosphorylation site(s) in PKC-η required for its interaction with CTLA-4, we mutated six predicted PKC-η phosphorylation sites, transfected these mutants into JTAg cells, a Jurkat cell derivative that does not express CD28 but expresses CTLA-4 (data not shown), and immunoprecipitated the transfected CTLA-4 proteins. Upon costimulation with anti-CD3 mAb and CD86-Fc recombinant protein, we found that mutations of amino acid residues S^{28} and S^{32} in the C2

domain, or S^{317} in the V3 domain of PKC-η abolished the interaction with CTLA-4 (Fig. 5a); as a control, mutation of three other phosphorylation sites (S^{327}, T^{656} or S^{675}) did not affect this interaction (Fig. 5a). Thus, phosphorylation of S^{28} and S^{32} or S^{317} in PKC-η is critical for the interaction with CTLA-4.

In order to determine whether the association between PKC-η and CTLA-4 is required for the suppressive function of T_{reg} cells, we generated bone marrow (BM) chimeric mice by retrovirally reconstituting *Prkch*$^{-/-}$-FIG BM cells with wild-type PKC-η or a mutant (PKC-η-S28A, S32A) that does not interact with CTLA-4. The retroviral vector used coexpressed a non-signaling rat CD2 to allow isolation of transduced T cells. Transduced T_{reg} cells ($rCD2^+GFP^+CD45.2^+$) from chimeric mice were sorted and assayed for their ability to suppress the *in vivo* homeostatic proliferation of cotransferred naïve $CD45.1^+$ T cells. Unlike T_{reg} cells expressing wild-type PKC-η, T_{reg} cells reconstituted with PKC-η-S28A, S32A were incapable of suppressing naïve T cell proliferation in the spleens and lymph nodes of adoptively transferred recipients (Fig. 5b-d).

To map the critical motif within the cytoplasmic tail of CTLA-4 that is required for the interaction with PKC-η, we mutated four conserved tail residues, *i.e*., a membrane proximal positively charged motif ($K^{188}XXKKR^{193}$), a proline-rich motif ($P^{205, 206, 209}$) and two tyrosine residues (Y^{201} or Y^{218}). We found that mutation of the positively charged $K^{188}XXKKR^{193}$ motif, as well as complete deletion of the CTLA-4 cytoplasmic tail (Δ183-223) greatly reduced the association with PKC-η; in contrast, mutations of the conserved tyrosine residues or the proline-rich motif did not affect the interaction (Fig. 5e). This membrane proximal motif is highly conserved throughout evolution from fish to primates (Supplementary Fig. 4a). Partial truncation of the cytoplasmic tail of CTLA-4 (Δ192-223), which left intact nine membrane proximal residues, including K^{188} and K^{191}, resulted in a residual association with PKC-η, which, however, was weaker than that displayed by full-length CTLA-4 (Supplementary Fig. 4b). Interestingly, T_{reg} cells expressing CTLA-4 with a similar incomplete truncation of the cytoplasmic tail were reported to retain suppressive activity[23, 24]. We also found that the interaction between CTLA-4 and PKC-η was not affected by PP2, an inhibitor of Src-family kinases (data not shown), consistent with the lack of effect of Y^{201} or Y^{218} CTLA-4 tail mutations on this interaction. Taken together, these results reveal that the CTLA-4-PKC-η interaction is necessary for the suppressive function of T_{reg} cells, thereby implicating PKC-η in a signaling axis linking CTLA-4 to T_{reg}-cell mediated suppression.

Impaired APC dissociation and CD86 depletion by *Prkch*$^{-/-}$ T_{reg} cells

In comparison to T_{eff} cells, T_{reg} cells preferentially form aggregates with APCs[4, 25], and this is due in part to the higher expression of adhesion molecules such as LFA-1[26] and neuropilin-1[27] on T_{reg} cells. Such T_{reg} cell-APC engagement has been implicated as a potential suppression mechanism, by allowing T_{reg} cells to effectively compete with T_{eff} cells in engaging APCs and, thus, inhibiting T_{eff} cell activation[25]. However, activation of LFA-1 and its conversion to a high affinity state, as measured by adhesion to its ligand, ICAM-1, was intact in *Prkch*$^{-/-}$ T_{reg} cells (Supplementary Fig. 5). Similarly, wild-type and *Prkch*$^{-/-}$ T_{reg} cells expressed similar levels of neuropilin-1, CD39 and CD73 (data not

shown), the latter two representing cell surface molecules that have been implicated in T_{reg} cell-mediated suppression through an adenosine-dependent action[28].

To elucidate the signaling mechanism potentially responsible for the PKC-η-mediated suppression, we performed a phosphoproteomic analysis of wild-type *vs.* *Prkch*$^{-/-}$ T_{reg} cells and found that PAK2 and GIT2, two components of a focal adhesion complex that promotes focal adhesion disassembly and, hence, cellular motility[29, 30], were significantly hypophosphorylated in *Prkch*$^{-/-}$ T_{reg} cells (Supplementary Fig. 6a). A complex of these two proteins together with the guanine nucleotide exchange factor αPIX was found to translocate to the T cell IS and to be required for optimal T_{eff} cell activation[31]. Moreover, CTLA-4 immunoprecipitates from anti-CD3- plus -CTLA-4-costimulated wild-type T_{reg} cells contained not only PKC-η, but also GIT2, αPIX and PAK kinase (Fig. 6a). These proteins were also present in PKC-η immunoprecipitates (data not shown). Of note, recruitment of this complex was unique to CTLA-4 costimulation, because the association of the GIT-PIX-PAK complex with CTLA-4 was barely above background level when the cells were costimulated with anti-CD3 plus - CD28 mAbs (Supplementary Fig. 6b). Thus, this particular signaling event is not shared between CTLA-4 and CD28. Furthermore, the activating phosphorylation of PAK kinases was dramatically reduced in *Prkch*$^{-/-}$ T_{reg} cells (Fig. 6b), indicating impaired activation of this complex.

Given the impaired PAK activation, and because PAK kinase was found to be required for TCR-induced transcriptional activation of NFAT and the CD28 response element (which includes an NF-κB-binding site) in Jurkat T cells[31, 32], we also examined whether *Prkch*$^{-/-}$ T_{reg} cells display impaired activation of these transcription factors following costimulation with anti-CD3ε plus -CTLA-4 mAbs. In these conditions we observed a severe defect in NFATc1 and NF-κB activation in the *Prkch*$^{-/-}$ T_{reg} cells (Fig. 6c).

Because the PAK2-GIT2 complex promotes cellular motility through focal adhesion disassembly[29, 30], we investigated if the defective activation of the GIT-PIX-PAK complex in *Prkch*$^{-/-}$ T_{reg} cells might result in a more stable conjugation of *Prkch*$^{-/-}$ T_{reg} cells with APCs. We noticed that the efficiency of conjugation between *Prkch*$^{-/-}$ T_{reg} cells and APCs was significantly higher by comparison to APC conjugates of wild-type T_{reg} cells (Fig. 6d), suggesting that in *Prkch*$^{-/-}$ T_{reg} cells, impaired activation of the GIT-PIX-PAK complex leads to defective breaking of T_{reg} cell-APC contacts.

If *Prkch*$^{-/-}$ T_{reg} cells display impaired dissociation from engaged APCs due to defective activation of the GIT-PIX-PAK complex, this defect may be expected to translate into reduced ability of *Prkch*$^{-/-}$ T_{reg} cells to serially engage new APCs, which, in turn, could result in reduced suppressive activity. This prediction is based on findings that T_{reg} cells can capture CD80 and CD86 molecule from APCs, a process that depletes the ligands required for CD28 costimulation of T_{eff} cells[15] and, thus, considered as a potential mechanism of contact-dependent T_{reg} cell-mediated suppression. To address this possibility, we tested the ability of wild-type *vs.* *Prkch*$^{-/-}$ T_{reg} cells to deplete CD86 from cocultured $CD45.2^{+}CD11c^{+}$ APCs as an indirect measure of APC engagement by the T_{reg} cells. wild-type and *Prkch*$^{-/-}$ T_{reg} cells were equally capable of depleting CD86 from these APCs (Fig. 6e, left panel). However, upon subsequent addition of a second pool of APCs, distinguished

from the first APC population by their CD45.1 expression, *Prkch*$^{-/-}$ T_{reg} cells had a significant delay in their ability to deplete CD86 from these newly introduced APCs, as indicated by the fact that it took them ~4-fold longer time (~16 *vs*. ~4 h) to execute the same level of CD86 depletion as that accomplished by wild-type T_{reg} cells (Fig. 6e, right panel). This observation supports the notion that the relative inefficiency of *Prkch*$^{-/-}$$T_{reg}$ cells to serially engage new APCs and, hence, to effectively deplete APC-expressed CD86, could account, at least in part, for their reduced suppressive activity. Importantly, our findings imply that a T_{reg} cell-intrinsic, CTLA-4-PKC-η-dependent signaling mechanism is required in order to manifest the cell-extrinsic suppressive function of CTLA-4 toward T_{eff} cells.

DISCUSSION

We report a novel interaction of CTLA-4 with PKC-η and preferential IS localization of PKC-η in T_{reg} cells upon their activation. Moreover, PKC-η and its CTLA-4 association were required for the contact-dependent suppressive function of T_{reg} cells, albeit not for their development. Although *Prkch*$^{-/-}$ T_{reg} cells displayed defective suppressive activity in a conventional *in vitro* suppression assay and in *in vivo* homeostatic proliferation and anti-tumor immunity models, they could still inhibit the development of autoimmune colitis. Our findings provide two potential explanations for these apparently discrepant observations. First, enhanced expansion of *Prkch*$^{-/-}$ T_{reg} cells in the inflammatory bowel environment, which was particularly noticeable in the mLN of recipient mice, could compensate for their reduced intrinsic suppressive function. Second, T_{reg} cells use various mechanisms of suppression and the relative importance of each mechanism depends on the environment and the context of the immune response. For example, similar to *Prkch*$^{-/-}$ T_{reg} cells, *Ctla4*$^{-/-}$ T_{reg} cells suppress the development of colitis through intact compensatory expression of IL-10[33], and we found that *Prkch*$^{-/-}$ T_{reg} cells expressed normal levels of IL-10. Thus, the CTLA-4-associated PKC-η-dependent suppressive pathway that we describe here may be less relevant in T_{reg} suppressive mechanisms that do not depend on T_{reg} cell-APC contact but, rather, on soluble mediators. If our observations of a dispensable role of PKC-η in T_{reg} cell protection against colitis can be extended to other autoimmune disease models, this would suggest that strategies that selectively inhibit PKC-η or its association with CTLA-4 may disable T_{reg} cells from inhibiting anti-tumor immunity without affecting their ability to protect against autoimmune diseases, a notion with important potential translational implications.

The T_{reg} cell defect revealed by our study may explain the increased cytokine production and higher amounts of serum IgE and autoantibodies in *Prkch*$^{-/-}$ mice, although intrinsic hyperactivity of the T_{eff} cells in these mice could also contribute to this increase. Nevertheless, it is interesting to note that mice with a Treg-specific deletion of *Ctla4* display similar increases in cytokine, IgE and autoantibody amounts[14], reinforcing the notion of a functionally relevant link between CTLA-4 and PKC-η at the level of T_{reg} cell-mediated suppression.

The recruitment of a GIT-PIX-PAK complex to CTLA-4 (and PKC-η) upon TCR plus CTLA-4 (but not CD28) costimulation of Treg and its impaired activation in *Prkch*$^{-/-}$ T_{reg} cells suggest a potential mechanism underlying their impaired suppressive activity, based on

previous findings that this macromolecular complex is required for the disassembly of focal adhesions in neurons and epithelial cells[29, 30] Given the reported localization of this complex to the T cell IS and its importance for T cell activation[31], it is possible that the TCR-activated GIT-PIX-PAK complex destabilizes T cell-APC contacts, thereby promoting conversion of the mature, concentric IS into an unstable IS (*i.e.*, kinapse), which is important for the motility of T cells and their ability to serially engage new APCs[34]. In the context of contact-dependent, T_{reg} cell-mediated suppression, increased stability of T_{reg} cell-APC conjugates and the concomitant reduction in their ability to serially engage new APCs would be translated to impaired overall suppressive activity. Consistent with this notion, we found that *Prkch*$^{-/-}$ T_{reg} cells form more efficient contacts with APCs in comparison with their wild-type counterparts and, furthermore, these *Prkch*$^{-/-}$ T_{reg} cells displayed a reduced ability to deplete CD86 from a second set of added APCs, likely a reflection of impairment in their disengagement from the first set of APCs. When considered at the population level and the relatively long time during which T_{reg} cells have the opportunity to engage APCs, this effect could translate into an overall reduction in CD86 depletion and, consequently, reduced T_{reg} cell suppression. Hence, our findings identify a T_{reg} cell-intrinsic signaling mechanism consisting of a CTLA-4-bound PKC-η-GIT-PIX-PAK complex, which plays a role in promoting the cell-extrinsic suppressive function of T_{reg} cell-expressed CTLA-4 on T_{eff} cells.

The biology of CTLA-4 is complex and its mechanisms of action in T cells are still incompletely understood. This complexity reflects, to a large extent, the fact that CTLA-4 is expressed both in T_{eff} cells where it functions in a cell-autonomous manner in *cis* to inhibit their activation, and in T_{reg} cells where it operates in a cell-non-autonomous manner in *trans* to dampen T_{eff} cell responses[17, 18, 35]. Earlier studies did not distinguish between these functions, but with the conditional deletion of *Ctla4* in T_{reg} cells only, it became evident that CTLA-4 expression by T_{reg} cells is in most (but not all) cases important for their suppressive function through depletion of CD80 and CD86 from APCs[14, 15, 36].

Ctla4$^{-/-}$ mice display fatal lymphoproliferative disorder characterized by the systemic infiltration of pathogenic self-reactive T cells[37, 38]. Although *Prkch*$^{-/-}$ mice displayed moderate lymphadenopathy, increase in memory-activated T cells and cytokine expression, and elevated IgE and autoantibodies at a relatively young age, they lived into adulthood (~1 year) with no gross signs of pathology (data not shown). Several functional disparities could account for these different phenotypes. First, CTLA-4 inhibits thymocyte negative selection[39] and, as a result, *Ctla4*$^{-/-}$ mice harbor autoreactive T cells that cause tissue damage[40]. However, thymic selection is largely intact in the absence of PKC-η[22], suggesting that the lack of overt autoreactivity and lymphoproliferation in *Prkch*$^{-/-}$ mice might limit the self-destructive nature of the hyperactive *Prkch*$^{-/-}$ T_{eff} cells. Second, the inhibitory effect of CTLA-4 is mediated by a combination of non-mutually exclusive mechanisms consisting of T_{reg} cell-intrinsic as well as T_{eff} cell-intrinsic mechanisms, and both mechanisms can cooperate to dampen T_{eff} cell responses. Third, our findings strongly suggest that the intrinsic ability *Prkch*$^{-/-}$ T_{reg} cells to deplete CD86 from APCs by transendocytosis (which depends on the CTLA-4extracellular domain) is intact, while only the newly described signaling function of CTLA-4, *i.e.*, the dissociation of T_{reg} cells from

APCs mediated by the PKC-η-GIT-PIX-PAK complex (which depends on the CTLA-4 cytoplasmic domain), is impaired. In contrast, T_{reg} cells from germline *Ctla4*$^{-/-}$ mice or Foxp3-Cre conditional *Ctla4*$^{-/-}$ mice lack both of these CTLA-4 functions.

Our findings of altered APC engagement and presumed reduced motility of *Prkch*$^{-/-}$ T_{reg} cells may be related to the reported ability of CTLA-4 to reverse the TCR stop signal and promote the motility of T_{eff} cells, possibly via LFA-1 activation[41, 42]. In contrast, T_{reg} cells were found to be resistant to the CTLA-4-induced reversal of the TCR stop signal, resulting in longer contact times with APCs[43], a scenario that would lead to lower overall T_{reg} cell motility and less frequent serial encounters with new APCs. However, we did not observe a defect in LFA-1 expression or activation in *Prkch*$^{-/-}$ T_{reg} cells and, furthermore, while LFA-1 promotes the formation of a stable IS, our findings point to a defect at a later stage, *i.e.*, disassembly of the IS in the *Prkch*$^{-/-}$ T_{reg} cells.

The successful clinical use of anti-CTLA-4 heralded a new era of cancer immunotherapy by targeting immunosuppression[44]. In many tumor tissues, infiltrating T_{reg} cells restrict the function of T_{eff} cells and, therefore, inhibiting critical T_{reg} cell signaling molecules that are important for their function could lead to enhanced antitumor responses[45]. Here, we showed that phosphorylated PKC-η is recruited to the T_{reg} cell IS and is associated with the cytoplasmic tail of CTLA-4, and demonstrated the critical importance of this association for the contact-dependent suppressive activity of T_{reg} cells. Hence, the CTLA-4-PKC-η axis could represent a key therapeutic target for T_{reg} cell-dependent suppression in controlling cancer.

METHODS

Antibodies (Abs) and reagents

mAbs specific for mouse CD3 (clone 145-2C11), CD28 (clone 37.51), or CTLA-4 (clone UC10-4B9) were purchased from Biolegend, as were flourophore-conjugated anti-CD4 (Clone GK1.5), -CD8 (53-6.7), -Foxp3 (Clone FJK-16s), -CD25 (Clone PC61), -CD44 (Clone IM7) and –GITR (Clone DTA-1) mAbs. Anti-human CD3 mAb (OKT3) was purified in-house. Polyclonal anti-PKC-θ (sc-212), anti-PKC-η (C-15 and sc-215), anti-PAK (N-20 and sc-882), anti-NFATc1 (7A6), anti-lamin B (M-20), and anti-α-tubulin (TU-02) Abs were obtained from Santa Cruz Biotechnology. Anti-p65 (NF-κB), anti-GIT2 and -αPIX Abs were obtained from Cell Signaling Technology. Anti-Foxp3 Abs (clone 150D/E4 for immunoblotting and clone FJK-16s for flow cytometry) were purchased from eBiosciences. Alexa-647-conjugated anti-mouse Ig and Alexa-555-conjugated anti-rabbit Ig were obtained from Molecular Probes. Digitonin was obtained from EMD Chemicals. Calf intestinal alkaline phosphatase was purchased from New England Biolabs. Recombinant CD86-Fc was previously described[46].

Plasmids

Plasmids of full-length human *Prkch* and mouse *Ctla4* were generated via PCR amplification and cloned into the pEF4/HisC expression vector or pMIG retroviral vector, respectively. *Prkch* and *Ctla4* point mutations were generated using Quikchange II Site-

directed Mutagenesis Kit (Stratagene). *Ctla4* mutants with cytoplasmic tail deletions (amino acid 183-223 and 192-223) were generated via PCR amplification.

Mice and primary cell cultures

C57BL/6 (B6; CD45.2$^+$), B6.SJL (CD45.1$^+$) and *Prkch*$^{-/-}$ (CD45.2$^+$)[22] mice were housed and maintained under specific pathogen-free conditions, and manipulated according to guidelines approved by the LIAI Animal Care Committee and the Animal Care and Use Committee of The Scripps Research Institute. The *Prkch*$^{-/-}$mice are now available from the Jackson Laboratories (B6.Cg-Prkch<tm1.1Gasc>/J). *Foxp3-IRES-eGFP* (FIG) mice were obtained from the Jackson Lab. *Prkch*$^{-/-}$ × *Foxp3-IRES-eGFP* (*Prkch*$^{-/-}$-FIG) mice[16] were generated by crossing FIG and *Prkch*$^{-/-}$ mice[22]. CD4$^+$ T cells were isolated by anti-CD4 (BD Biosciences) positive selection, and were cultured in RPMI-1640 medium (Mediatech, Inc.) supplemented with 10% heat-inactivated fetal bovine serum, 2 mM glutamine, 1 mM sodium pyruvate, 1 mM MEM nonessential amino acids, and 100 U/ml each of penicillin G and streptomycin (Life Technologies).

Immunoprecipitation and immunoblotting

Simian virus 40 large T antigen-transfected human leukemic Jurkat T cells (JTAg) and MCC-specific hybridoma T cells were described previously[9]; these cell lines have not been recently STR profiled but tested negative for mycoplasma contamination. JTAg cells in logarithmic growth phase were transfected with plasmid DNAs by electroporation and incubated for 48 h. Transfected cells were stimulated with an anti-human CD3 (OKT3) mAb and recombinant CD86-Fc in the presence of a cross-linking Ab for 5 min. Cell lysis in 1% NP-40 lysis buffer (50 mM Tris-HCl, 50 mM NaCl, 5 mM EDTA), immunoprecipitation, and immunoblotting were carried out as previously described[9].

Enzyme-linked immunoabsorbent assay (ELISA)

Serum IgE was quantified using capture and biotinylated mAbs from CALTAG Laboratories, as previously described[47]. Autoantibodies specific for double-stranded DNA (dsDNA) and histone were determined using plates coated with salmon sperm DNA (Life Technologies) or calf thymus histone (Roche), respectively. Detection was carried out using biotinylated anti-mouse IgG, streptavidin conjugated HRP, and ABTS substrates (Bio-Rad). Relative Ig serum levels were calculated by dividing the absorbance values of experimental samples by the negative control values.

Isolation of mRNA, cDNA synthesis and real-time PCR

Total RNA was extracted from sorted CD4$^+$GFP$^-$ and CD4$^+$GFP$^+$ cells of FIG mice using the RNeasy kit (Qiagen). RNA was used to synthesize cDNA by the SuperScript III FirstStrand cDNA synthesis kit (Life Technologies). Gene expression was determined using real-time PCR with iTaq SYBR Green (Bio-Rad) in the presence of the following primer sets for mouse *Ctla4* (Forward: 5’ ACTCATGTACCCACCGCCATA 3’; Reverse: 5’ GGGCATGGTTCTGGATCAAT 3’), *Prkch* (Forward: 5’ CAAGCATTTTACCAGGAAGCG 3’; Reverse: 5’ TGTTTCCCAAATACTCCCCAG 3’)

and the housekeeping gene β-actin (*ACTB*). Relative gene expression levels were determined in triplicates and calculated using the $2^{-\Delta\Delta Ct}$ and normalized to the level of *ACTB*.

Microscopy

$CD4^+$ T cells were purified from AND-Tg *Rag2*$^{-/-}$ mice and stimulated by immobilized anti-CD3ε (145-2C11; 10 μg/ml) and anti-CD28 (PV-1; 1 μg/ml) in the presence of mouse recombinant IL-2 (10 ng/ml) and human recombinant TGFβ (5 ng/ml) for 3 d. The cells were retrovirally transduced with eGFP-tagged mouse PKC-θ or PKC-η for 24 h one day after the initial stimulation. On d 4 or later, the cells were sorted on a FACSAria (BD) to obtain homogenous population of highly GFP^+ cells, which were maintained in culture. B cells purified from B10. BR mice and stimulated by LPS (Difco; 10 μg/ml) plus MCC (1 μM) were added to the cultured T cells for 1 d. Dead cells were removed by Lympholite-M (Cedarlane), and the $CD4^+$ T_{reg} cells were prestained by DyLight650-labeled anti-TCRβ (H57) Fab, conjugated with MCC-pulsed LPS-stimulated B cells for 5-10 min, fixed with 2% PFA, and imaged by confocal microscopy (Leica SP5) with ProLong gold antifade reagent with DAPI (Molecular Probes).

In vitro suppression assay

FACS-sorted naïve $CD4^+CD62L^+$ T_{eff} cells were labeled with 5 μM of CellTrace Violet according to the manufacturer's protocol (Life Technologies). $CD11c^+$ splenic DCs were purified according to the manufacturer's instructions (Miltenyi Biotech). Labeled T_{eff} cells (2×10^4) and splenic DCs (5×10^3) were cocultured for 3 days with $CD4^+GFP^+$ T_{reg} cells ($0.125\text{-}4 \times 10^4$) sorted from wild-type or *Prkch*$^{-/-}$ FIG mice in the presence of an anti-mouse CD3 mAb.

Homeostatic expansion model

Naïve $CD4^+CD62L^+$ cells from congenic B6. SJL and $CD4^+GFP^+T_{reg}$ cells from wild-type and *Prkch*$^{-/-}$ FIG mice were sorted using ARIA Cell Sorter (BD Biosciences). Two $\times 10^6$ naïve cells were transferred i.v. alone or together with 0.5×10^6 $CD4^+GFP^+$ T_{reg} cells into *Rag1*$^{-/-}$ mice; this was done blind and assigned randomized with no pre-established inclusion/exclusion criteria. Mice were euthanized 7-10 days post-transfer. Spleens, pLN and mLN were harvested and each population was independently analyzed by flow cytometry. To achieve reasonable power, at least 5 mice/group (15 mice/experiment) were used. Additional mice were added to experiments as appropriate.

B16 melanoma model

Splenocytes from wild-type B6 mice were depleted of $CD25^+$ cells using biotinylated anti-CD25 mAb (clone PC61, eBiosciences) and streptavidin-conjugated beads (BD Biosciences). $CD4^+GFP^+$ T_{reg} cells were FACS-sorted from wild-type or *Prkch*$^{-/-}$ FIG mice. 15×10^6 CD25-depleted splenocytes were adoptively transferred alone or together with 0.5×10^6 wild-type or *Prkch*$^{-/-}$ $CD4^+GFP^+$ T_{reg} cells into recipient *Rag1*$^{-/-}$ mice; this was done blind and assigned randomized with no pre-established inclusion/exclusion criteria. Two $\times 10^5$ B16-F10 melanoma cells were inoculated intradermally on the right shaved flanks the next day. Tumor size was measured using an electronic dial caliper 2-3

times/week[14]. To achieve reasonable power, at least 5 mice/group (15 mice/experiment) were used. Additional mice were added to experiments as appropriate.

BM chimeras

Full-length human wild-type or S28A, S32A mutated *Prkch* were subcloned into a modified pMIG retroviral vector containing IRES and non-signaling rat CD2 gene (lacking the cytoplasmic tail). BM chimeras were produced in irradiated B6 mice as previously described[9]. Briefly, BM cells were flushed from the femurs and tibias of *Prkch*$^{-/-}$-FIG mice that have been pretreated with 5-fluorouracil to enrich for stem cells. BM cells were cultured in DMEM media (Mediatech, Inc.) containing 10% FBS, IL-3 (20 ng/ml), IL-6 (25 ng/ml) and stem cell factor (SCF;100 ng/ml). Retroviral infections were carried out for 2 consecutive days. 1×10^6 infected BM cells were intravenously injected into irradiated B6 mice. Analyses were performed 10-12 weeks post-reconstitution to determine cells coexpressing GFP (for Foxp3 expression) and rat CD2 (for transgene expression) using anti-rCD2 mAb (clone OX-34, Biolegend). Cells were pooled from spleens and peripheral LN of 4-5 chimeric mice, and enriched for CD4$^+$ cells. GFP$^+$rCD2$^+$double positive T_{reg} cells were sorted on an ARIA Cell Sorter, and their *in vivo* suppressive function was analyzed in a homeostatic expansion assay as described above.

T_{reg} cell-APC coculture

GFP$^+$ T_{reg} cells (5×10^4) from wild-type or *Prkch*$^{-/-}$ FIG mice were cultured with CellTrace Violet-labeled splenic CD11c$^+$ APCs (5×10^4) for the indicated times. Cells were carefully collected with cut tips and immediately assayed on an LSRII flow cytometer to determine double-positive (GFP$^+$Violet$^+$) conjugates. For CD86 depletion experiment, T_{reg} cells (5×10^4) were cultured with CD45.2$^+$CD11c$^+$ splenic APCs (2.5×10^4) for 9 h and, after which CD45.1$^+$CD11c$^+$ splenic APC (2.5×10^4) from B6.SJL mice were added for another 9 h. Cells were collected and stained with fluorophore-conjugated Abs specific for CD11c, Annexin V, CD4, CD86, I-A^b, CD45.1, or CD45.2.

SILAC and phosphoproteomic analysis

wild-type and *Prkch*$^{-/-}$ FIG naïve CD4$^+$ T cells were differentiated into iT_{reg} cells as described above in regular RPMI-1640 medium or medium supplemented with ^{13}C, ^{15}N labeled lysine and arginine for SILAC labeling. FACS-sorted GFP$^+$ T_{reg} cells were left unstimulated or stimulated with anti-CD3 plus -CTLA-4 mAbs for 5 min, wild-type and *Prkch*$^{-/-}$ FIG cell lysates were mixed at a 1:1 ratio, and 300 μg of the protein mixture was precipitated with 5x volume of cold acetone. Following centrifugation at 14,000 × *g* (10 min at 4°C), protein pellets were solubilized and reduced with 100 mM Tris-HCl/8 M urea/5 mM tris(2-carboxyethyl)phosphine. Cysteine was alkylated with 10 mM iodoacetamide. The solution was diluted 1:4 and digested with 5 μg of trypsin at 37°C overnight. Digestion was terminated by adding 10% acetonitrile and 2% formic acid, and the resulting peptides were subjected to TiO_2 phosphopeptide enrichment as described[48]. Briefly, phosphopeptides were bound to the TiO_2 resin, and eluted with 250 mM NH_4HCO_3, pH 9. Enriched phosphopeptides were analyzed by the MudPIT LC-MS/MS method[49]. MS analysis was performed using an LTQ-Orbitrap Velos mass spectrometer (Thermo Fisher). A cycle of one

full-scan mass spectrum (300-1800 m/z) at a resolution of 60,000 followed by 20 data dependent MS/MS spectra at a 35% normalized collision energy was repeated continuously throughout each step of the multidimensional separation.

MS data were analyzed by the Integrated Proteomics Pipeline - IP2 (Integrated Proteomics Applications; http://www.integratedproteomics.com/). The tandem mass spectra were searched against EBI IPI mouse target/decoy protein database. Protein false discovery rates were controlled below 1% for each sample. In ProLuCID database search, the cysteine carboxyamidomethylation was set as a stable modification, and phosphorylation on serine, threonine, or tyrosine was configured as differential modification. Peptide quantification was performed by Census software, in which the isotopic distributions for both the unlabeled and labeled peptides were calculated and this information was then used to determine the appropriate m/z range from which to extract ion intensities. Phosphopeptides were further evaluated with IP2 phospho analysis module, which computes Ascore[50] and Debunker score[51].

Statistical analysis

Statistical analyses were performed using, unless otherwise stated, ANOVA with *post-hoc* Bonfferoni's corrections. Unless otherwise indicated, data represent the mean ± s.e.m, with $P < 0.05$ considered statistically significant.

Supplementary Material

Refer to Web version on PubMed Central for supplementary material.

Acknowledgments

The authors would like to acknowledge H. Cheroutre and Y.-C. Liu for helpful discussions. The authors would also like to acknowledge the excellent services provided by the Flow Cytometry Core Unit at LIAI, as well as the Animal Husbandry Units at LIAI and TSRI. This is publication number 1552 from the La Jolla Institute for Allergy and Immunology and 21923 from The Scripps Research Institute. This work was supported by NIH grants CA35299 (AA), GM065230 (NRJG), and P01AI089624 (MK). KFK was supported by LIAI-T1D-CRF 2012 Fellowship and Young Investigator Award #270056 from the Melanoma Research Alliance.

References

1. Bennett CL, et al. The immune dysregulation, polyendocrinopathy, enteropathy, X-linked syndrome (IPEX) is caused by mutations of FOXP3. Nat Genet. 2001; 27:20–21. [PubMed: 11137993]
2. Fontenot JD, Gavin MA, Rudensky AY. Foxp3 programs the development and function of CD4+CD25+ regulatory T cells. Nat Immunol. 2003; 4:330–336. [PubMed: 12612578]
3. Hori S, Nomura T, Sakaguchi S. Control of regulatory T cell development by the transcription factor Foxp3. Science. 2003; 299:1057–1061. [PubMed: 12522256]
4. Zanin-Zhorov A, et al. Protein kinase C-theta mediates negative feedback on regulatory T cell function. Science. 2010; 328:372–376. [PubMed: 20339032]
5. Collins AV, et al. The interaction properties of costimulatory molecules revisited. Immunity. 2002; 17:201–210. [PubMed: 12196291]
6. Yokosuka T, et al. Spatiotemporal basis of CTLA-4 costimulatory molecule-mediated negative regulation of T cell activation. Immunity. 2010; 33:326–339. [PubMed: 20870175]
7. Teft WA, Kirchhof MG, Madrenas J. A molecular perspective of CTLA-4 function. Annu Rev Immunol. 2006; 24:65–97. [PubMed: 16551244]

8. Kong KF, Altman A. In and out of the bull's eye: protein kinase Cs in the immunological synapse. Trends Immunol. 2013; 34:234–242. [PubMed: 23428395]
9. Kong KF, et al. A motif in the V3 domain of the kinase PKC-theta determines its localization in the immunological synapse and functions in T cells via association with CD28. Nat Immunol. 2011; 12:1105–1112. [PubMed: 21964608]
10. Kim JK, et al. Impact of the TCR signal on regulatory T cell homeostasis, function, and trafficking. PLoS One. 2009; 4:e6580. [PubMed: 19668367]
11. Park SG, et al. T regulatory cells maintain intestinal homeostasis by suppressing gammadelta T cells. Immunity. 2010; 33:791–803. [PubMed: 21074460]
12. Chuck MI, Zhu M, Shen S, Zhang W. The role of the LAT-PLC-gamma1 interaction in T regulatory cell function. J Immunol. 2010; 184:2476–2486. [PubMed: 20130215]
13. Spitaler M, Emslie E, Wood CD, Cantrell D. Diacylglycerol and protein kinase D localization during T lymphocyte activation. Immunity. 2006; 24:535–546. [PubMed: 16713972]
14. Wing K, et al. CTLA-4 control over Foxp3+ regulatory T cell function. Science. 2008; 322:271–275. [PubMed: 18845758]
15. Qureshi OS, et al. Trans-endocytosis of CD80 and CD86: a molecular basis for the cell-extrinsic function of CTLA-4. Science. 2011; 332:600–603. [PubMed: 21474713]
16. Haribhai D, et al. Regulatory T cells dynamically control the primary immune response to foreign antigen. J Immunol. 2007; 178:2961–2972. [PubMed: 17312141]
17. Tang Q, Bluestone JA. The Foxp3+ regulatory T cell: a jack of all trades, master of regulation. Nat Immunol. 2008; 9:239–244. [PubMed: 18285775]
18. Josefowicz SZ, Lu LF, Rudensky AY. Regulatory T cells: mechanisms of differentiation and function. Annu Rev Immunol. 2012; 30:531–564. [PubMed: 22224781]
19. Matsuda JL, et al. Systemic activation and antigen-driven oligoclonal expansion of T cells in a mouse model of colitis. J Immunol. 2000; 164:2797–2806. [PubMed: 10679123]
20. Collison LW, et al. The inhibitory cytokine IL-35 contributes to regulatory T-cell function. Nature. 2007; 450:566–569. [PubMed: 18033300]
21. Shimizu J, Yamazaki S, Sakaguchi S. Induction of tumor immunity by removing CD25+CD4+ T cells: a common basis between tumor immunity and autoimmunity. J Immunol. 1999; 163:5211–5218. [PubMed: 10553041]
22. Fu G, et al. Protein kinase C eta is required for T cell activation and homeostatic proliferation. Sci Signal. 2011; 4:ra84. [PubMed: 22155788]
23. Tai X, et al. Basis of CTLA-4 function in regulatory and conventional CD4+ T cells. Blood. 2012; 119:5155–5163. [PubMed: 22403258]
24. Kataoka H, et al. CD25(+)CD4(+) regulatory T cells exert in vitro suppressive activity independent of CTLA-4. Int Immunol. 2005; 17:421–427. [PubMed: 15724061]
25. Onishi Y, Fehervari Z, Yamaguchi T, Sakaguchi S. Foxp3+ natural regulatory T cells preferentially form aggregates on dendritic cells in vitro and actively inhibit their maturation. Proc Natl Acad Sci U S A. 2008; 105:10113–10118. [PubMed: 18635688]
26. Tran DQ, et al. Analysis of adhesion molecules, target cells, and role of IL-2 in human FOXP3+ regulatory T cell suppressor function. J Immunol. 2009; 182:2929–2938. [PubMed: 19234188]
27. Sarris M, Andersen KG, Randow F, Mayr L, Betz AG. Neuropilin-1 expression on regulatory T cells enhances their interactions with dendritic cells during antigen recognition. Immunity. 2008; 28:402–413. [PubMed: 18328743]
28. Borsellino G, et al. Expression of ectonucleotidase CD39 by Foxp3+ Treg cells: hydrolysis of extracellular ATP and immune suppression. Blood. 2007; 110:1225–1232. [PubMed: 17449799]
29. Zhao ZS, Manser E, Loo TH, Lim L. Coupling of PAK-interacting exchange factor PIX to GIT1 promotes focal complex disassembly. Mol Cell Biol. 2000; 20:6354–6363. [PubMed: 10938112]
30. Lucanic M, Cheng HJ. A RAC/CDC-42-independent GIT/PIX/PAK signaling pathway mediates cell migration in C. elegans. PLoS Genet. 2008; 4:e1000269. [PubMed: 19023419]
31. Phee H, Abraham RT, Weiss A. Dynamic recruitment of PAK1 to the immunological synapse is mediated by PIX independently of SLP-76 and Vav1. Nat Immunol. 2005; 6:608–617. [PubMed: 15864311]

32. Yablonski D, Kane LP, Qian D, Weiss A. A Nck-Pak1 signaling module is required for T-cell receptor-mediated activation of NFAT, but not of JNK. The EMBO journal. 1998; 17:5647–5657. [PubMed: 9755165]
33. Uhlig HH, et al. Characterization of Foxp3+CD4+CD25+ and IL-10-secreting CD4+CD25+ T cells during cure of colitis. J Immunol. 2006; 177:5852–5860. [PubMed: 17056509]
34. Dustin ML. T-cell activation through immunological synapses and kinapses. Immunol Rev. 2008; 221:77–89. [PubMed: 18275476]
35. Walker LS, Sansom DM. The emerging role of CTLA4 as a cell-extrinsic regulator of T cell responses. Nat Rev Immunol. 2011; 11:852–863. [PubMed: 22116087]
36. Read S, Malmström V, Powrie F. Cytotoxic T lymphocyte-associated antigen 4 plays an essential role in the function of Cd25+Cd4+ regulatory cells that control intestinal inflammation. J Exp Med. 2000; 192:295–302. [PubMed: 10899916]
37. Tivol EA, et al. Loss of CTLA-4 leads to massive lymphoproliferation and fatal multiorgan tissue destruction, revealing a critical negative regulatory role of CTLA-4. Immunity. 1995; 3:541–547. [PubMed: 7584144]
38. Waterhouse P, et al. Lymphoproliferative disorders with early lethality in mice deficient in Ctla-4. Science. 1995; 270:985–988. [PubMed: 7481803]
39. Buhlmann JE, Elkin SK, Sharpe AH. A role for the B7-1/B7-2:CD28/CTLA-4 pathway during negative selection. J Immunol. 2003; 170:5421–5428. [PubMed: 12759417]
40. Ise W, et al. CTLA-4 suppresses the pathogenicity of self antigen-specific T cells by cell-intrinsic and cell-extrinsic mechanisms. Nat Immunol. 2010; 11:129–135. [PubMed: 20037585]
41. Schneider H, et al. Reversal of the TCR stop signal by CTLA-4. Science. 2006; 313:1972–1975. [PubMed: 16931720]
42. Rudd CE. The reverse stop-signal model for CTLA4 function. Nat Rev Immunol. 2008; 8:153–160. [PubMed: 18219311]
43. Lu Y, Schneider H, Rudd CE. Murine regulatory T cells differ from conventional T cells in resisting the CTLA-4 reversal of TCR stop-signal. Blood. 2012; 120:4560–4570. [PubMed: 23047820]
44. Peggs KS, Quezada SA, Allison JP. Cancer immunotherapy: co-stimulatory agonists and co-inhibitory antagonists. Clin Exp Immunol. 2009; 157:9–19. [PubMed: 19659765]
45. Peggs KS, Quezada SA, Chambers CA, Korman AJ, Allison JP. Blockade of CTLA-4 on both effector and regulatory T cell compartments contributes to the antitumor activity of anti-CTLA-4 antibodies. J Exp Med. 2009; 206:1717–1725. [PubMed: 19581407]
46. Kim G, et al. Spontaneous colitis occurrence in transgenic mice with altered B7-mediated costimulation. J Immunol. 2008; 181:5278–5288. [PubMed: 18832683]
47. Becart S, et al. SLAT regulates Th1 and Th2 inflammatory responses by controlling Ca2+/NFAT signaling. J Clin Invest. 2007; 117:2164–2175. [PubMed: 17657315]
48. Wang H, et al. The interaction of CtIP and Nbs1 connects CDK and ATM to regulate HR-mediated double-strand break repair. PLoS Genet. 2013; 9:e1003277. [PubMed: 23468639]
49. Washburn MP, Wolters D, Yates JR 3rd. Large-scale analysis of the yeast proteome by multidimensional protein identification technology. Nat Biotechnol. 2001; 19:242–247. [PubMed: 11231557]
50. Beausoleil SA, Villen J, Gerber SA, Rush J, Gygi SP. A probability-based approach for high-throughput protein phosphorylation analysis and site localization. Nat Biotechnol. 2006; 24:1285–1292. [PubMed: 16964243]
51. Lu B, Ruse C, Xu T, Park SK, Yates J 3rd. Automatic validation of phosphopeptide identifications from tandem mass spectra. Anal Chem. 2007; 79:1301–1310. [PubMed: 17297928]

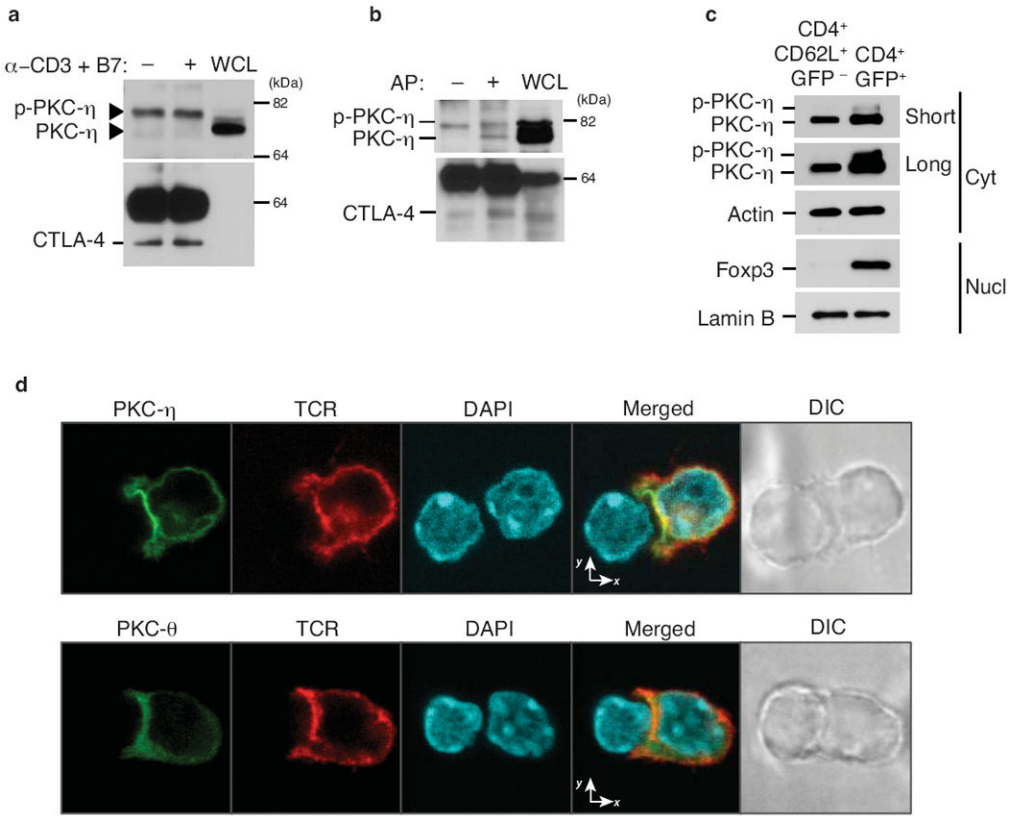

Figure 1.

IS recruitment and CTLA-4 interaction of PKC-η in T_{reg} cells. (**a**) Immunoblot analysis of T hybridoma cells left unstimulated (-) or stimulated (+) with anti-CD3 plus CD86-Fc for 5 min. CTLA-4 IPs (left and center lanes) or whole cell lysates (WCL) were immunoblotted with the indicated Abs. Arrowheads mark the two PKC-η species. (**b**) Immunoblot analysis of IPs (left and center lanes) or WCL (right lane) from T hybridoma cells stimulated with anti-CD3 plus CD86-Fc for 5 min. CTLA-4 IPs were left untreated (-) or treated with alkaline phosphatase (AP; +) prior to immunoblotting. (**c**) Immunoblot analysis of cytosol or nuclear fractions from sorted $CD4^+CD62L^+GFP^-$ (naïve) and $CD4^+GFP^+$ (**T_{reg}**) cells (2×10^6 each) from wild-type FIG mice. Data in (**a-c**) are representative of at least four experiments. (**d**) Confocal imaging of PKC-η (top row) or PKC-θ (bottom row) and TCRβ localization in *in vitro* differentiated iT_{reg} cells from AND TCR-Tg *Rag2*$^{-/-}$ mice, which were retrovirally transduced with eGFP-tagged mouse PKC-θ or PKC-η 1 d after anti-CD3 and -CD28 stimulation. Sorted GFP^+ T cells (~90% $FoxP3^+$ by intracellular staining; not shown) obtained on d 4 and stimulated for 5-10 min by conjugation with MCC-pulsed LPS-stimulated B cells were fixed and analyzed. eGFP-tagged PKC, TCR and nuclear DAPI staining are shown in green, red and blue, respectively. Images are representative of at least 100 cells collected from three independent experiments.

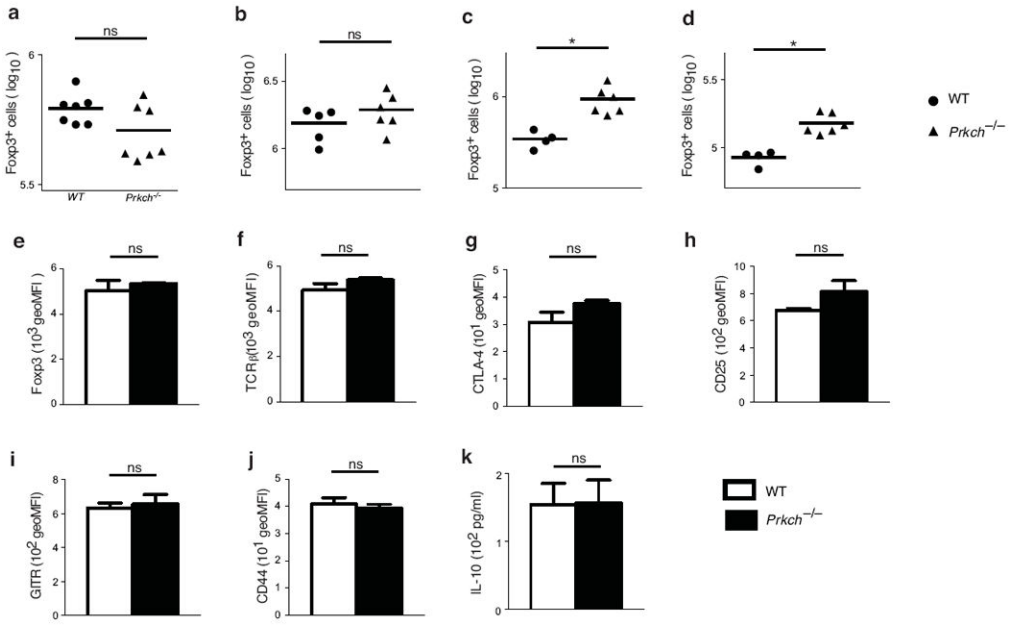

Figure 2.

Development of Foxp3$^+$ T$_{reg}$ cells is independent of PKC-η. (**a-d**) Cell counts (Log$_{10}$) of CD4$^+$Foxp3$^+$ cells from thymi (**a**), spleens (**b**), peripheral lymph nodes (pLN; **c**) and mesenteric lymph nodes (mLN; **d**) of 8-12 week-old wild-type or *Prkch*$^{-/-}$ mice determined by intracellular Foxp3 staining. Each data point represents a single mouse. ns, non significant; *$P < 0.05$. (**e-j**) Mean fluorescence intensity (MFI) of Foxp3 (**e**), TCRβ (**f**), CTLA-4 (**g**), CD25 (**h**), GITR (**i**) and CD44 (**j**) expression determined on gated CD4$^+$Foxp3$^+$-cells from wild-type or *Prkch*$^{-/-}$ mice. (**k**) IL-10 production (measured by ELISA) by CD4$^+$GFP$^+$ T$_{reg}$ cells from wild-type and *Prkch*$^{-/-}$ FIG mice, which were stimulated with plate-bound anti-CD3 mAb and CD86-Fc in the presence of IL-2 overnight. For description of FIG mice, see Fig. 3 and the corresponding text.

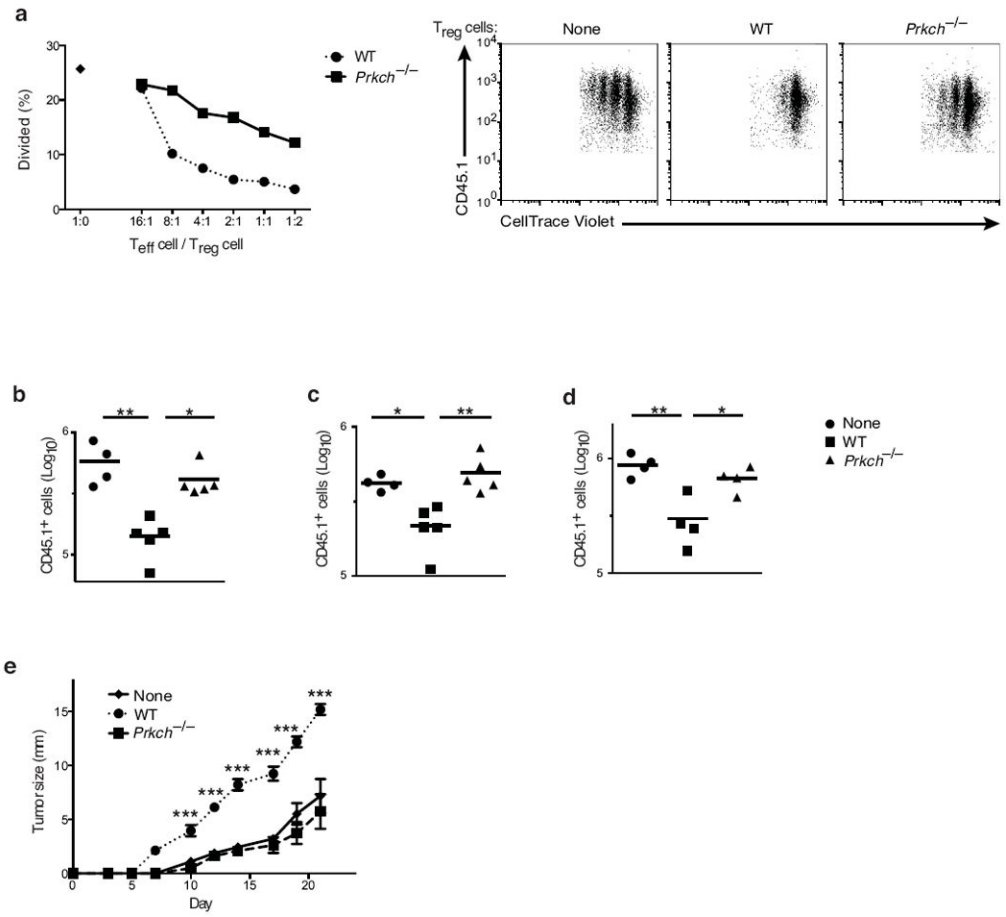

Figure 3.

Contact-dependent suppression by T_{reg} cells depends on PKC-η. (**a**) *In vitro* suppression assay measuring the proliferation of CellTrace Violet-labeled naïve B6 $CD4^+CD25^-$ T_{eff} cells cocultured in the absence (1:0) or presence of $Foxp3^+$ T_{reg} cells from wild-type or $Prkch^{-/-}$FIG mice at the indicated T_{eff}/T_{reg} cell ratios, and stimulated with anti-CD3 mAb and splenic DCs for 3 d. Percentages of CellTrace Violet-diluting T_{eff} cells were calculated (left panel). The three right panels show representative FACS dot plots of dye-diluting T_{eff} cells cultured with T_{reg} cells at a 1:1 ratio. Data are representative of at least five independent experiments. (**b-d**) *In vivo* homeostatic proliferation assay showing the number (Log_{10}) of B6.SJL $CD45.1^+$ naïve T cells recovered from spleens (**b**), pLN (**c**) or mLN (**d**) of recipient $Rag1^{-/-}$ mice 7 d after i.v. transfer of naïve cells (2×10^6) in the absence (none) or presence of FACS-sorted $CD4^+GFP^+$ T_{reg} cells ($.5 \times 10^6$) from FIG or $Prkch^{-/-}$-FIG mice. Each data point represents a single mouse. (**e**) Sequential measurements of B16-F10 melanoma growth in groups of $Rag1^{-/-}$ mice ($n \geq 5$), which received CD25-depleted B6 splenic cells (1.5×10^7; a source of T_{eff} cells) without or with 0.5×10^6 $CD4^+GFP^+$ T_{reg} cells from wild-type or $Prkch^{-/-}$ FIG mice, and were inoculated one day later with tumor cells (2×10^5). Tumor diameters along two perpendicular axes were measured 2-3 times/ week. $*P < 0.05$; $**P < 0.01$; $***P < 0.001$. This experiment is representative of at least three independent experiments.

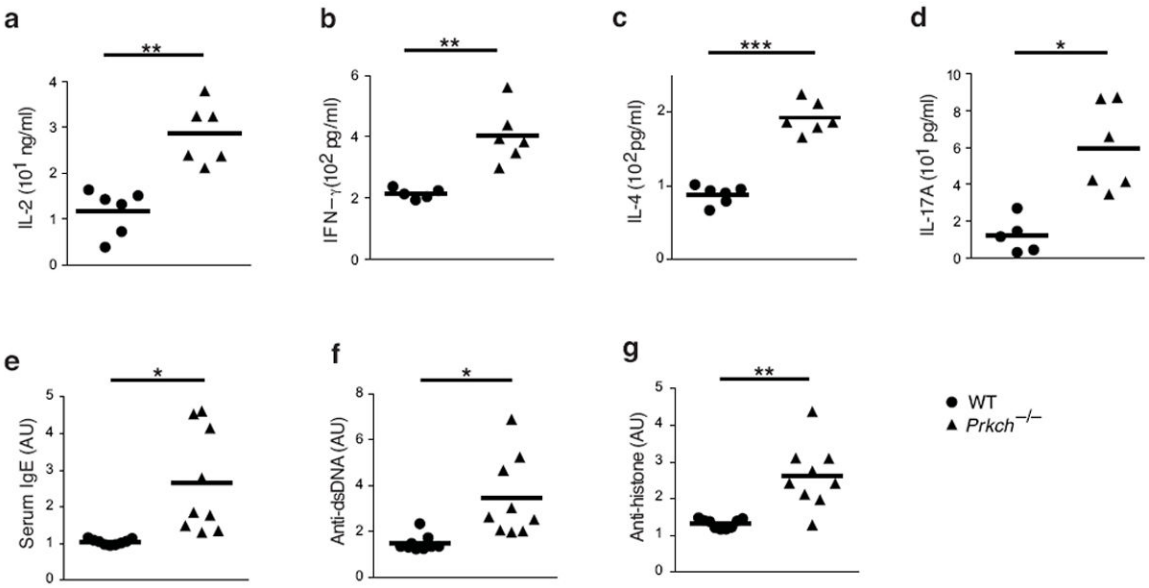

Figure 4. Cytokine production and serum antibody levels of WT *vs. Prkch*$^{-/-}$ mice

(**a-d**) Cytokine expression in culture supernatants of WT or *Prkch*$^{-/-}$ FACS-sorted CD44^{hi} T cells, which were stimulated with anti-CD3 plus -CD28 mAbs for 24 h and assayed by an ELISA for levels of IL-2 (**a**), IFNγ (**b**), IL-4 (**c**) and IL-17A (**d**). (**e-g**) Serum levels of IgE (**e**), anti-double stranded DNA (**f**) or anti-histone (**g**) antibodies in 8-12 week-old wild-type and *Prkch*$^{-/-}$ mice determined by an ELISA. Each data point represents a single mouse from two pooled experiments. **P* < 0.01 ***P* < 0.001; ****P* < 0.0001.

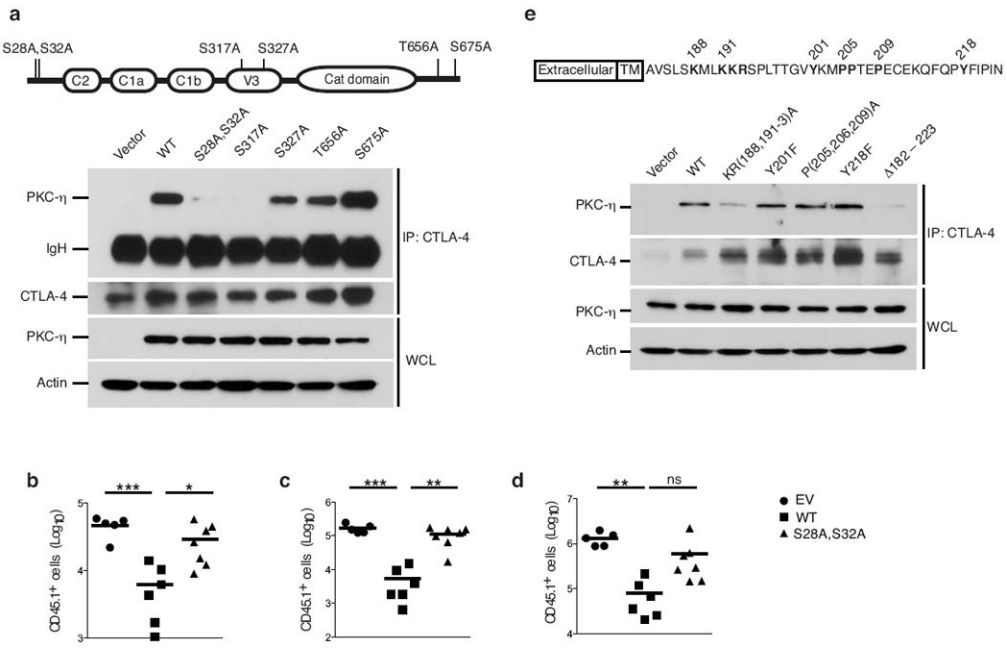

Figure 5.

Mapping and biological significance of the CTLA-4-PKC-η interaction sites. (**a**) Immunoblot analysis of CTLA-4 IPs or WCL from JTAg cells, which were cotransfected with the indicated PKC-η vectors plus wild-type CTLA-4 and stimulated as in Fig. 1a. IgH, heavy chain of the precipitating antibody. Schematic representation of human PKC-η and its phosphorylation sites is shown on top. Data are representative of at leas five independent experiments. (**b-d**) *In vivo* homeostatic proliferation assay performed as described in Fig. 3b-d showing the number (Log_{10}) of B6.SJL CD45.1$^+$ naïve T cells, which were recovered from spleens (**b**), pLN (**c**) or mLN (**d**) of recipient *Rag1*$^{-/-}$ mice 10 d post i.v. transfer of naive cells (2×10^6) in the absence (vector) or presence of FACS-sorted rCD2$^+$CD4$^+$GFP$^+$ T_{reg} cells ($.5 \times 10^6$). T_{reg} cells were derived from *Prkch*$^{-/-}$ BM mouse chimeras reconstituted with wild-type PKC-η or a CTLA-4 non-interacting PKC-η-S28A, S32A using retroviral pMIG-IRES-rCD2 vector. Each data point represents a single mouse. ns, non significant; *$P < 0.05$; **$P < 0.01$; ***$P < 0.001$. (**e**) Immunoblot analysis of CTLA-4 IPs or WCL from JTAg cells cotransfected with the indicated CTLA-4 vectors plus wild-type PKC-η, and processed as in (**a**). Schematic representation of mouse CTLA-4 is shown on top.

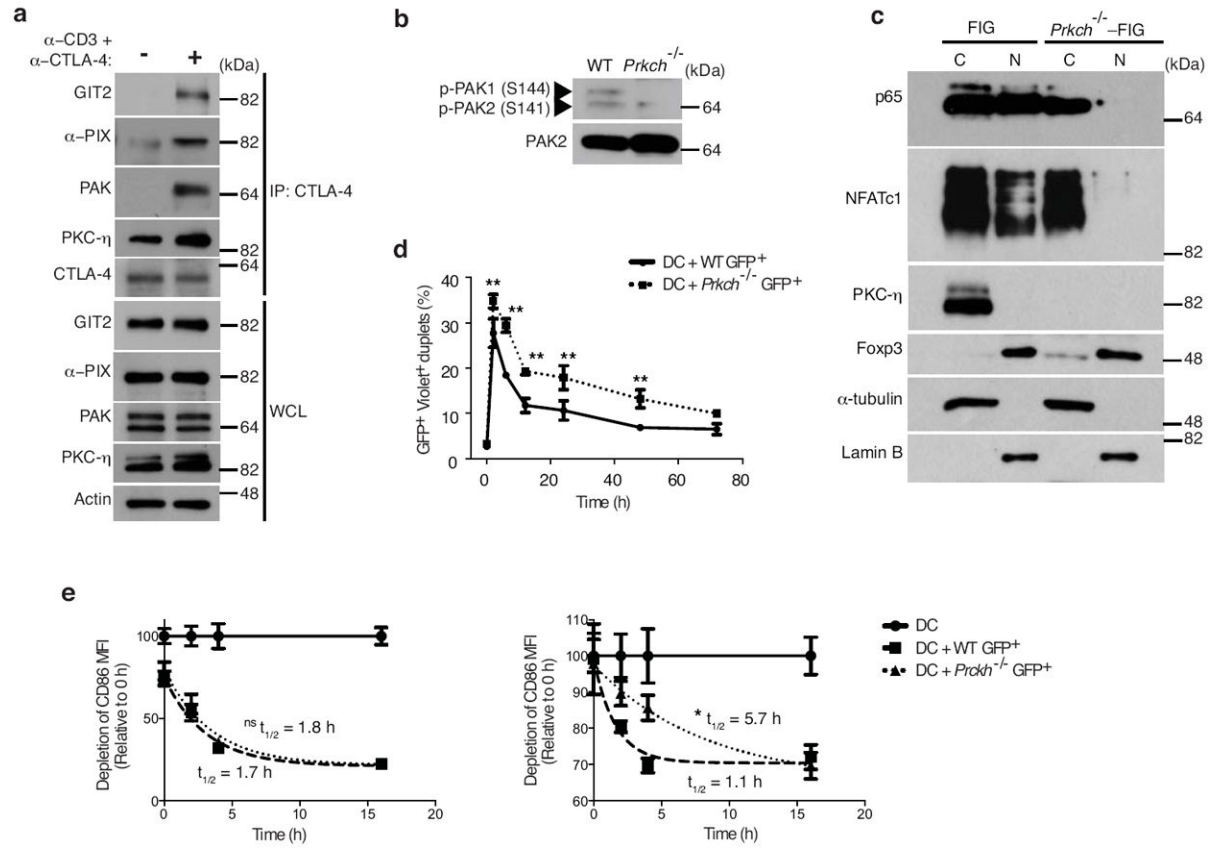

Figure 6.

CTLA-4-PKC-η recruits GIT-PIX-PAK complex and modulates T_{reg} cell-APC interaction. (**a**) Immunoblot analysis of cytosolic (C) and nuclear (N) fractions of FACS-sorted wild-type or *Prkch*$^{-/-}$ FIG CD4^{+}GFP^{+} T_{reg} cells, which were stimulated with anti-CD3ε plus -CTLA-4 mAbs for 5 min. (**b**) Immunoblot analysis of CTLA-4 IPs or WCL of FACS-sorted GFP^{+} T_{reg} cells derived from FIG mice and left unstimulated (-) or stimulated (+) with ani-CD3 plus anti-CTLA-4 antibodies for 5 min. (**c**) Expression of phospho-PAK and total PAK2 in lysates of CD4^{+}GFP^{+} T_{reg} cells from wild-type or *Prkch*$^{-/-}$ FIG mice determined by immunoblotting with the corresponding antibodies. (**d**) Conjugation assay measuring formation of cell doublets between FACS-sorted CD4^{+}GFP^{+} wild-type or *Prkch*$^{-/-}$ FIG T_{reg} and CellTrace Violet-labeled splenic DCs at different times during a 3 d coculture period in the presence of anti-CD3 mAb and IL-2. Percentages of GFP^{+} and Violet^{+} double-positive doublets are shown. **P* < 0.05; ***P* <0.001. (**e**) CD86 depletion from APCs cocultured in the absence (circles) or presence of FACS-sorted CD4^{+}GFP^{+} wild-type (squares) or *Prkch*$^{-/-}$ (triangles) FIG T_{reg} cells. A first set of CD45.2^{+} splenic DCs was cultured for 9 h in the presence of anti-CD3 mAb and IL-2 prior to the addition of a second set of CD45.1^{+} splenic DCs. The geometric mean fluorescence intensity of CD86 was enumerated on gated CD11c^{+} Annexin V^{-} CD45.2^{+} and CD11c^{+} Annexin V^{-} CD45.1^{+} cells, respectively. The $t_{1/2}$ values of CD86 decay curves were calculated using the GraphPad Prism™ program. This experiment is representative of three independent experiments. ns, non significant; **P* < 0.05.